Physics of the Solid State, 2023, Vol. 65, No. 2

05,01

Study of domain wall dynamics in GdFeCo using double high-speed photography

© K.N. Prabhakara, T.B. Shapaeva¶, V.V. Yurlov, K.A. Zvezdin, A.K. Zvezdin, C.S. Davies, A. Tsukamoto, A.I. Kirilyuk, Th. Rasing, A.V. Kimel

Lomonosov Moscow State University,
Moscow, Russia

¶ E-mail: shapaeva@mail.ru

Received October 25, 2022
Revised October 25, 2022
Accepted November 1, 2022

Using the technique of double high-speed photography method, we show that an external magnetic field triggers in GdFeCo domain wall motion with velocities up to 1.2 km/s. The domain wall velocity saturates with an increase of the driving magnetic field. Contrary to earlier experiments on iron garnets, we did not succeed to detect any effect of femtosecond laser pulses on the domain wall velocity, even if the pulses were strong enough to reverse magnetization.

Keywords: ferrimagnetism, domain wall dynamics, high-speed photography method, Faraday effect.

DOI: 10.21883/PSS.2023.02.55407.506

1. Introduction

Recently, there has been a significant amount of interest in not only domains, but also in domain walls (DW) in order to solve important problems of spintronics, such as creation of new logical systems and memory devices [1–4], which operation is based on controlled DW motion. Currently, there are several methods to control this displacement, including spin-polarized current, geometrical structures, and magnetic field. Recently, it was demonstrated that electric current can trigger the motion of domain walls with very high speeds of up to 5.7 km/s [5–7]. Experiments with optics also have demonstrated the possibility of control the DW position using light [8,9]. In addition, recent research has shown the promising potential of integration of optics and spintronics, the optospintronics, as one of methods to process magnetic information in the future [10,11]. To put it in another way, studying the DW dynamics is the basis for improvement of characteristics of real device prototypes in the future.

The discovery of all-optical magnetization reversal [12–14] has demonstrated the possibility to control the magnetic order using light in ferromagnetic compounds, which are composed of rare earth elements and transition metals. In addition, experiments for temperature dependence of DW motion speed in such compounds have shown an acceleration of the domain wall in the region of angular momentum compensation temperature (T_A) [15,16]. Thus, the investigation of DW dynamics, as well as studying the effect of powerful optical pulses on the speed of domain wall in GdFeCo compounds is an actual task.

In this study we used a method that combines the double high-speed photography and the pump-probe method to investigate the dynamics of domain walls in the GdFeCo compound at room temperature, as well as the effect of light on the moving domain wall.

2. Experiment

The dynamics of domain wall in GdFeCo was investigated by means of the double high-speed photography method based on the Faraday effect [17]. In this work the double photography method with the use of femtosecond laser was combined with the pump-probe method [18]. We have used the following geometry in the experiment: probe pulse 1–pump pulse–probe pulse 2. This geometry allows not only studying the dynamics of domain wall in a transparent ferromagnetic, but also recording the effect of pump pulse on it. The idea of experiment with two probe pulses and one pump pulse is shown in Fig. 1. The pump and probe pulses had a duration of 70 fs and a wavelength of 400 and 800 nm, respectively. The delay between probe pulses was $\Delta t = 10$ ns.

Position of the single domain wall was stabilized using gradient magnetic field created by permanent magnets (Fig. 1, *a*). Value of the gradient magnetic field oriented normally to the sample plane was about 0.3 T/cm. In addition to the component directed along the z axis, gradient magnets created in-plane field $H_y^{\parallel} \sim 0.36$ T. Solenoids located on surfaces of the sample created a pulsed magnetic field oriented along the z axis($h_z^{\perp}$). We used this field to control dynamics of the DW. Amplitude of the field $h_z^{\perp}$ was from 80 to 230 mT at a pulse duration of 20 μs and its leading edge of 20 ns. Probe pulses were arriving on the sample normal to its surface (Fig. 1, *b*). The pump pulse was oriented at a small angle to the sample normal and arrived to the sample 1 ns after the first probe pulse (Fig. 1, *b, d*). The beam diameter of the pump pulse was about 50 μm. The direction of magnetization was controlled using the magneto-optic Faraday effect. The first and the second probe pulses created opposite contrast images of the two-domain structure (Fig. 1, *c*). The light band resulted from the superposition of these images represents the distance passed by the domain wall over the time between probe pulses. The combination of the double photography method and the pump-probe method allows not only studying the

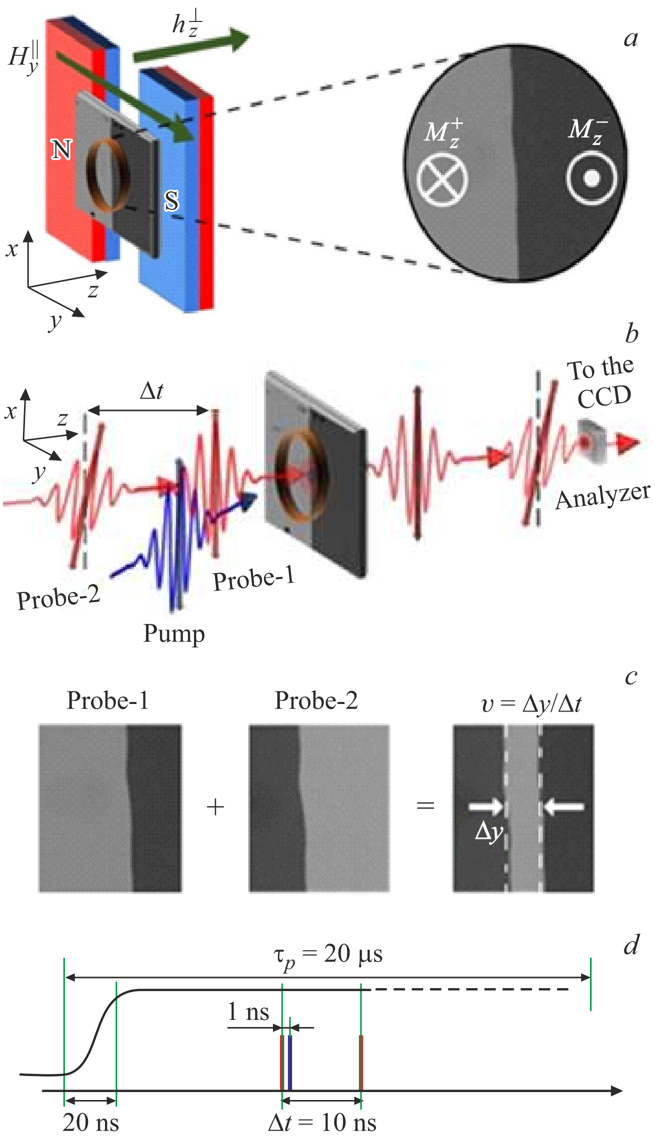

Figure 1. Combination of the double high-speed photography and the pump-probe method. (*a*) Creation of a single domain wall in the sample. M_z^+ and M_z^- — directions of magnetization in adjacent domains, $H_y^{||}$ — permanent magnetic field normal to the plane of domain wall, which is created by permanent magnets. $h_z^{\perp}$ — pulsed magnetic field that controls the dynamics of the domain wall. (*b*) Relative positions of pump and probe pulses. Two optical probe pulses separated by a time interval Δt, illuminate the dynamic domain wall. The pump pulse acts on the moving wall 1 ns after the first probe pulse. (*c*) Photos of the domain structure obtained with the help of each probe beams separately and sum of these images. Width of the light band in the last photo Δy is equal to the distance passed by the domain wall over the time interval between two probe pulses Δt [18]. (*d*) Relative positions of the magnetic field pulse with a duration of τ_p and light pulses in the geometry of probe pulse 1 — pump pulse — probe pulse 2.

DW dynamics, but comparing the DW dynamics withing the region of pump pulse impact and out of this region. All measurements were carried out in the strobe mode with a repetition frequency of 10 Hz at room temperature.

The under-study compound of rare-earth (*Re*) and transition metal (TM) had the following composition: $Gd_{23}Fe_{67.94}Co_{9.06}$ and was grown in the form of a thin film in the glass/SiN (5 nm)/*Re*-TM structure (20 nm)/SiN (60 nm). It is worth to note, that the composition of samples in our experiments was the same as in [15]. The material has demonstrated a uniaxial perpendicular magnetic anisotropy, which allowed observing the domain structure of the sample with the help of the Faraday effect. As it was noted by the authors of [15], the compensation point in the material is $T_M \sim 220$ K, the angular momentum compensation temperature is $T_A \sim 310$ K.

The DW starts moving under the action of the pulsed magnetic field. Fig. 2, *a* shows the dependence of DW displacement from the equilibrium on the time passed after the start of action of the magnetic field pulse with an amplitude of $h_z^{\perp} \sim 83$ mT. The wall is speeded up gradually up the maximum speed, then it slows down and stops. The quite long time of the domain wall acceleration to the maximum speed (about 0.4 μs) is related to the inductance of the coils that create the pulsed magnetic field [19]. The dependence represented in Fig. 2, *a* allows determining the interval of time during which the speed of domain wall motion remained constant and maximum at a fixed amplitude of the pulsed magnetic field. Further measurements of the wall motion speed at different amplitudes of magnetic fields were carried out 0.5 μs after the start of field pulse action, when the domain wall achieved its maximum speed.

Fig. 2, *b* shows images of moving DW recorded by means of the double photography method. Width of the light band in the image represents the distance passed by the DW over the time between two probe pulses. Value of the magnetic field that puts the DW in motion is specified under the images. In all photos the wall moves from top to bottom. It should be noted that both top and bottom edges of the light band in all photos is quite even, no broadening of the dynamic domain wall is observed.

Using the photos similar to those presented in Fig. 2 *b*, the dependence of DW speed on the pulsed magnetic field shown in Fig. 2, *c* was obtained. Accuracy of the wall speed determining was at least 0.05 km/s. The DW speed increases with growth of the magnetic field $h_z^{\perp}$ and achieves saturation under fields higher than 250 mT, as shown in Fig. 2, *c*. The blue solid line corresponds to the data defined by the $v(h_z^{\perp})$ function:

$$v(h_z^{\perp}) = \frac{\mu h_z^{\perp}}{\sqrt{1 + \left(\frac{\mu h_z^{\perp}}{c}\right)^2}} \qquad (1)$$

here $\mu \sim 9.2$ km/s/T is mobility of the DW, the saturation speed c ~ 1.5 km/s. Equation (1) was already used before to describe the $v(h_z^{\perp})$ dependence by authors of [17,20,21]. It should be noted, that the mobility of the domain wall at 290 K measured by authors of [15] is ~ 10 km/s/T, which corresponds to the mobility in our experiment.

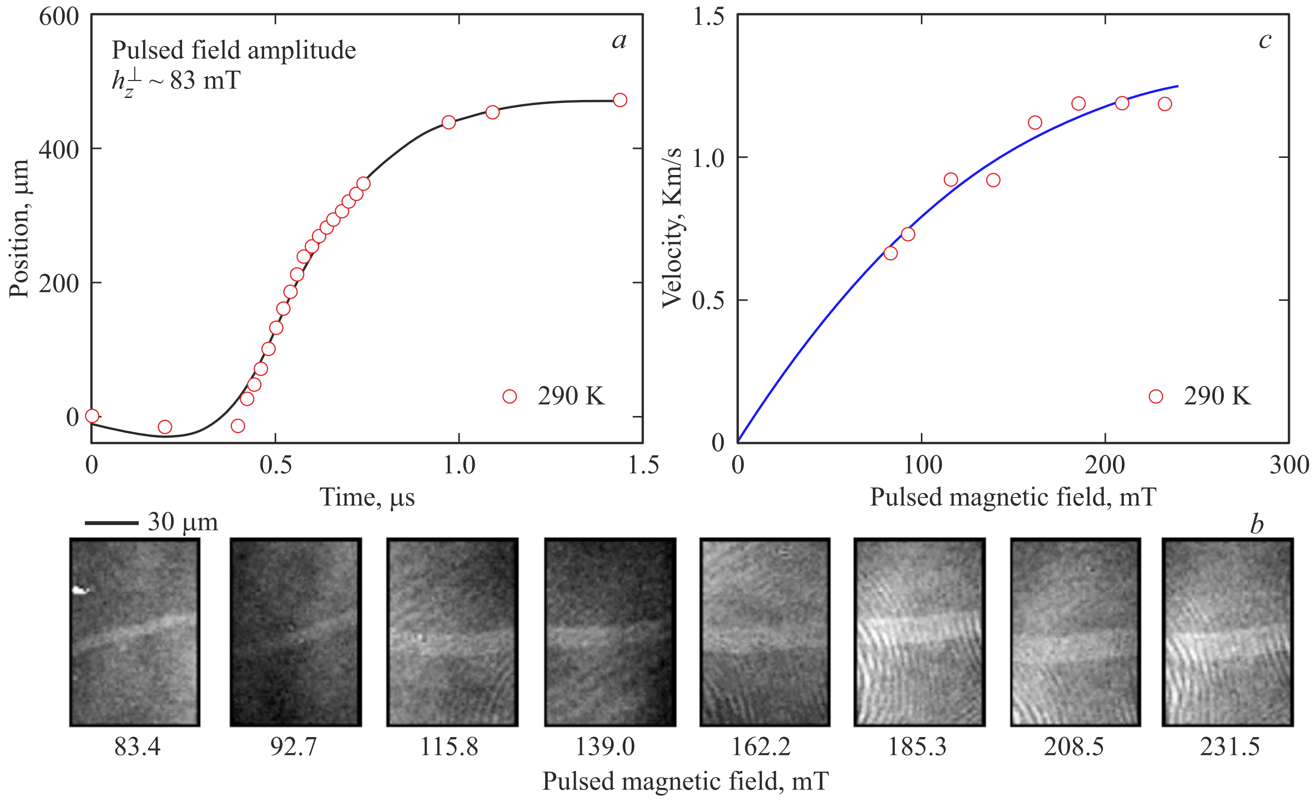

Figure 2. DW dynamics in GdFeCo at room temperature. (a) Dependence of the domain wall displacement x on time at a pulse field amplitude of $h_z^{\perp} \sim 83$ mT. Black solid line represents the general trend. (b) Double photos of the dynamic domain wall recorded $0.5\,\mu$s after the start of the magnetic field pulse action. White band on the image represents the distance passed by the domain wall for different amplitudes of the pulsed field $h_z^{\perp}$. (c) Dependence of the domain wall speed on the amplitude of pulsed magnetic field $h_z^{\perp}$. Blue solid line is the curve calculated by equation (1).

Using equation (7) from [22], the speed of saturation c can be estimated:

$$c = \bar{\gamma}_{eff}\sqrt{\frac{2A}{\chi_{\perp}}}. \qquad (2)$$

Assuming that $A \sim 2 \cdot 10^{-7}$ erg/cm, $\bar{\gamma}_{eff} = 1.73 \cdot 10^7$, $\chi_{\perp} \sim 2 \cdot 10^{-3}$, we get $c \sim 1.7$ km/s, which is qualitatively corresponds to the experimentally observed value.

It must be noted that sometimes on the path of the domain wall motion a domain is formed on local defects of the sample, and the size of this domain increases under the action of the pulsed field controlling the wall motion. At the same time, motion speeds of the straightline domain wall and the domain formed on a defect were equal to each other. A similar effect was observed earlier when investigating the dynamics of domain walls in films of ferrite garnets in large in-plane fields.

Fig. 3 shows double photos obtained with the use of the following configuration: probe pulse *1* — pump pulse — probe pulse *2*. The domain wall moves from top to bottom. The impact of laser pulse on the wall motion was investigated at different powers of the exciting pulse. When studying all-optical magnetization reversal, the authors of [12,13] have shown that an energy of 2.6 mJ/cm^2 is sufficient for a local magnetization reversal

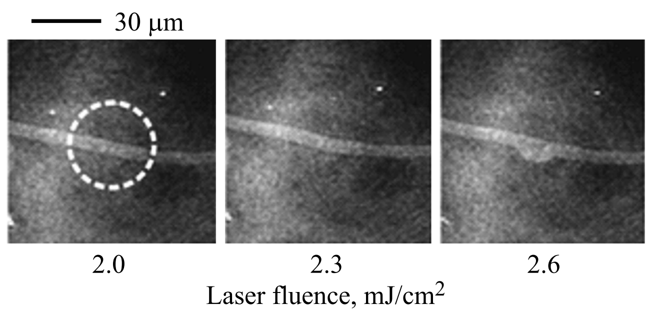

Figure 3. Dynamics of domain wall in the presence of pump pulses with different power. The domain wall moves from top to bottom at a speed of $v_0 \approx 0.66$ km/s. Light band represents the distance passed by the wall over the time between two probe pulses. The pump pulse acts on the moving domain wall inside the white dashed circle.

using an optical pulse. This pulse changes the magnetization in the exposed region, a new domain occurs, that can be combined over time with a domain, which magnetization is directed along the field controlling the domain wall motion. This can be seen in the right photo in Fig. 3 as a broadening of the light band. Since

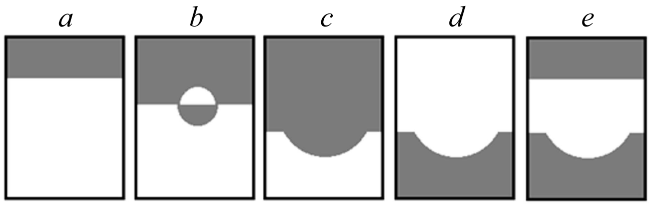

Figure 4. Scheme illustrating behavior of the domain structure under optical magnetization reversal. The domain wall moves from top to bottom. (*a*) The first probe pulse records the two-domain structure. (*b*) Optical magnetization reversal after the pump pulse action 1 ns after the action of the first probe pulse. Domains of magnetization reversal — dark and light semi-circles. (*c*) Under the action of the external magnetic field the area of dark domain increases, which results in disappearance of the small light domain. This type of domain structure can be recorded by means of the second probe pulse, which lags behind the first one by 10 ns. To obtain double photo, the contrasts of images from the first and the second beams are opposite: Fig. 4, *c* and 4 *d* have opposite contrasts. (*e*) Double photo of the dynamic domain wall resulted from superposition of figures 4, *a* and 4, *d*.

such a broadening can be different in different places of the sample, it is probably related to the arrangement of defects on which new domains are nucleated, and is not related to the pump pulse impact. Hence, even under an impact of the optical pulse with an energy sufficient for magnetization reversal, the exciting pulse does not impact directly on the motion of the domain wall, and causes just an optical magnetization reversal, which can be misinterpreted as an acceleration of the domain wall. Since a similar result is observed regardless the polarization of the exciting pulse, this phenomenon has a thermal nature.

Fig. 4 shows a scheme that explains the observed phenomenon. The domain wall moves from top to bottom. Fig. 4, *a* shows a two-domain structure recorded with the help of the first probe pulse. Fig. 4, *b* shows a domain structure after the action of the pump pulse. Here the domains with reversed magnetization are shown as dark and light semi-circles. Since the external magnetic field promotes broadening of the dark domain, the little light domain disappears and the domain structure has the form shown in Fig. 4, *c*. This is exactly the type of domain structure that can be recorded by means of the second probe pulse, which, as it was mentioned above, lags behind the first one by 10 ns. To obtain a double photo, contrasts of the images recorded from the first and the second beams are opposite: Fig. 4, *c* and 4, *d* have opposite contrast. As a result of superposition of figures 4, *a* and 4, *d* we get Fig. 4, *e*, which is a double photo of the dynamic domain wall. Fig. 4, *e* is similar to the photo shown in Fig. 3, that corresponds to a pump pulse energy of 2.6 mJ/cm^2. Thus, it is clear that in the case of similar scenario the broadening of the light band in the photo is not indicative of DW acceleration under the action of optical pulse.

3. Discussion of results

The GdFeCo compound is a ferrimagnetic with two sublattices [12]. A well-known example of this type of material is the bismuth-containing ferrite garnet, where the dynamics of domain walls is investigated in sufficient detail [17,21,23]. For such materials the $v(h_z^{\perp})$ dependence linearly increases at the initial section, includes a region with negative differential mobility, and increases again. Thus type of dependence behavior in GdFeCo was observed by authors of [15], while maximum speed of the DW motion at room temperature was not greater than 1 km/s. The presence of a decreasing section in the $v(h_z^{\perp})$ dependence is related to the change in the internal structure of the wall, which is resulted from the generation of magnetic vortices inside it: vertical and horizontal Bloch lines [17]. To suppress the generation of vortices and stabilize structure of the domain wall, in the process of domain walls dynamics investigation in ferrite garnets a plane magnetic field was used with its orientation normal to the plane of the wall [21,23]. In this case the $v(h_z^{\perp})$ dependence changed its behavior: now the initial linearly increasing section evolved to saturation and there was no decreasing section. To put it another way, while without a plane magnetic field the dynamics of the domain wall in ferromagnetic materials can be described by the Landau–Lifshitz equation, in the presence of the plane field it is reasonable to use the model of easy-plane ferromagnetic [24].

In this experiment, to stabilize the initial position of the domain wall we used a gradient field created by permanent magnets, which, along with the inductance of the magnetic field normal to the plane of the sample, had a component laid in the sample plane normal to the plane of the wall. It was noted before, that value of this component was 0.36 T, and it was sufficient to suppress the generation of magnetic vortices and save structure of the domain wall, therefore no decreasing section of the $v(h_z^{\perp})$ dependence was recorded. It should be noted, that the saturation of the $v(h_z^{\perp})$ dependence in GdFeCo was not observed before.

The absence of laser-induced effects on the moving DW in GdFeCo is highly surprising. Taking into account the density of laser pulse energy, it can be estimated how much the sample temperature changes under the action of the optical excitation. Using the value of specific heat capacity of $\sim 2.7\,\mathrm{MJ/(m^3 \cdot K)}$ [25], the absorption coefficient at 800 nm equal to $\sim 0.25\,\mathrm{mn}^{-1}$ [26], the spot diameter of the pump pulse of $\sim 50\,\mu$, the change in temperature ($\Delta T_{\max}$) can be estimated. With the maximum pump pulse energy of $\sim 2.6\,\mathrm{mJ/sm^2}$ the $\Delta T_{\max} \sim 33\,\mathrm{K}$. Thus, the density of energy should be sufficient to overcome the compensation temperature T_A ($T_A \sim 310\,\mathrm{K}$ [15]) in the excited domain of the sample, where DW speed increases by 1.5–3 times [15].

To explain the observed phenomenon, the following scenario was proposed. The action of the pump pulse results in heating of the excited domain, in which the DW speeds up [15]. The local change in temperature changes the material properties, such as anisotropy, magnetization, and gyromagnetic ratio [15,27]. Hence, it can change the internal structure of the DW. It is known, that an increase in the wall speed results in the magnetization vector getting out of its plane [23,24], thus promoting the generation of pair of magnetic vortices that move along the DW in opposite directions [17]. It was already mentioned before that the presence of vortices inside the dynamic DW decreases its speed.

In a two-sublattice ferrimagnetic the effective gyromagnetic ratio γ_{eff} depends on magnetization and gyromagnetic ratios of each sublattice. In the GdFeCo compound there is a rare-earth sublattice (RE) and a transition metal sublattice (TM). With the help of equation (3) from [27], γ_{eff} can be represented as

$$\gamma_{eff}(T) = \frac{M_{RE}(T) - M_{TM}(T)}{\frac{M_{RE}(T)}{|\gamma_{RE}|} - \frac{M_{TM}(T)}{|\gamma_{TM}|}}, \quad (3)$$

where M_{RE}, M_{TM} — magnetization of sublattices, γ_{RE}, γ_{TM} — gyromagnetic ratios of sublattices. Since magnetizations of each sublattice depend on temperature, γ_{eff} is a function of temperature, as well. The value of γ_{eff} increases considerably near the angular momentum compensation temperature [27]. The gyroscopic force that defines the motion of vortices inside the DW depends on the wall speed and gyromagnetic ratio [28]:

$$F_g = \frac{M_s}{\gamma}[\mathbf{v_n} \times \mathbf{z}] \quad (4)$$

here M_s — magnetization of saturation, v_n — projection of DW speed on the normal to the wall plane, and z — unit vector normal to the sample plane. As a consequence, it is expected that the gyroscopic force acting on the magnetic vortices, which occurred inside the DW, will be considerably reduced in a region closer to T_A. In addition, the suppression of Bloch lines generation is promoted by the presence of the in-plane compomemt of the gradient magnetic field [17].

Thus, the local heating of the sample promotes DW speeding up, which promotes generation of magnetic vertices, that slowing down it. To put it another way, the absence of the laser-induced effect near T_A may be a consequence of the balance between two opposite effects.

It should be noted, that a similar mechanism of change in the internal structure of DW under the action of the pump pulse was proposed in [18] to explain the slowing down of DW in the film of ferrite garnet under the action of optical pulse. However, in the film of ferrite garnet the speed of DW motion did not exceed 0.6 km/s and slowing down of DW was observed, if the speed of wall was less than 0.5 km/s, i.e. in the case when one of competing mechanisms prevailed. In this experiment with the GdFeCo compound the speed of DW was from 0.6 to 1.2 km/s.

4. Conclusion

The method of double high-speed photography was used to investigate the dynamics of DW in the GdFeCo compound ferrimagnetic at room temperature. It was shown that the speed of DW motion increases and saturates at a level of 1.2 km/s. The speed saturation is caused by the stabilization of the domain wall structure in the presence of a plane magnetic field and, as a consequence, the absence of the DW thin structure — magnetic vertices. In addition, experiments have shown the absence of pump pulse effect on the dynamic domain wall, regardless of the fact that power of this pulse was sufficient for magnetization reversal. This is probably caused by the balance of opposite effects: acceleration of DW due to the local heating and generation of magnetic vertices in the heated domain. A similar phenomenon was observed before under certain conditions in films of ferrite garnets [18].

Acknowledgments

The authors would like to thank T. Toonen, S. Symin, K. Berkhut for technical support, as well as O. Tretyakov for useful discussions.

Conflict of interest

The authors declare that they have no conflict of interest.

References

[1] D.A. Allwood, G. Xiong, C.C. Faulkner, D. Atkinson, D. Petit, R P. Cowburn. Science **309**, *5741*, 1688 (2005).
[2] D.A. Allwood, G. Xiong, M.D. Cooke, C.C. Faulkner, D. Atkinson, N. Vernier, R.P. Cowburn. Science **296**, *5575*, 2003 (2002).
[3] J.H. Franken, H.J. Swagten, B. Koopmans. Nature Nanotechnol. **7**, *8*, 499 (2012).
[4] S. Parkin, S.H. Yang. Nature Nanotechnology **10**, *3*, 195 (2015).
[5] T. Okuno, D.-H. Kim, S.-H. Oh, S.K. Kim, Y. Hirata, T. Nishimura, W.S. Ham, Y. Futakawa, H. Yoshikawa, A. Tsukamoto, Y. Tserkovnyak, Y. Shiota, T. Moriyama, K.-J. Kim, K.-J. Lee, T. Ono. Nature Electron. **2**, *9*, 389 (2019).
[6] D.-H. Kim, D.-Ho Kim, K.-J. Kim, K.-W. Moon, S. Yang, K.-J. Lee, S.K. Kim. JMMM **514**, *15*, 167237 (2020).
[7] K. Cai, Z. Zhu, J. M. Lee, R. Mishra, L. Ren, S.D. Pollard, P. He, G. Liang, K.L. Teo H. Yang. Nature Electron. **3**, 37 (2020).
[8] Y. Quessab, R. Medapalli, M.S. El Hadri, M. Hehn, G. Malinowski, E.E. Fullerton, S. Mangin. Phys. Rev. B **97**, 054419 (2018).
[9] T. Janda, P.E. Roy, R.M. Otxoa, Z. Soban, A. Ramsay, A.C. Irvine, F. Trojanek, M. Surynek, R.P. Campion, B.L. Gallagher, P. Nemec, T. Jungwirth, J. Wunderlich. Nature Commun. **8**, 15226 (2017).
[10] M.L.M. Lalieu, R. Lavrijsen, B. Koopmans. Nature Commun. **10**, *12*, 110 (2019).
[11] B. Zhang, Y. Xu, W. Zhao, D. Zhu, X. Lin, M. Hehn, G. Malinowski, D. Ravelosona, S. Mangin. Phys. Rev.Appl. **11**, 034001 (2019).
[12] C.D. Stanciu, F. Hansteen, A. V. Kimel, A. Kirilyuk, A. Tsukamoto, A. Itoh, T. Rasing. Phys. Rev. Lett. **99**, 047601 (2007).

[13] M.L. Lalieu, M.J. Peeters, S.R. Haenen, R. Lavrijsen, B. Koopmans. Phys. Rev. B **96**, 220411 (2017).
[14] Y. Xu, M. Hehn, W. Zhao, X. Lin, G. Malinowski, S. Mangin. Phys. Rev. B **100**, 064424 (2019).
[15] K.J. Kim, S.K. Kim, Y. Hirata, S.H. Oh, T. Tono, D.H. Kim, T. Okuno, W.S. Ham, S. Kim, G. Go, Y. Tserkovnyak, A. Tsukamoto, T. Moriyama, K.J. Lee, T. Ono. Nature Mater. **16**, *12*, 1187 (2017).
[16] L. Caretta, M. Mann, F. Büttner, K. Ueda, B. Pfau, C. M. Gunther, P. Hessing, A. Churikova, C. Klose, M. Schneider, D. Engel, C. Marcus, D. Bono, K. Bagschik, S. Eisebitt, G. S. Beach. Nature Nanotechnol. **13**, *12*, 1154 (2018).
[17] V.G. Bar'yakhtar, M.V. Chetkin, B.A. Ivanov, S.N. Gadetskii. Springer Tracts Mod. Phys. **129** (1994).
[18] K.H. Prabhakara, T.B. Shapaeva, M.D. Davydova, K.A. Zvezdin, A.K. Zvezdin, C.S. Davies, A. Kirilyuk, Th. Rasing, A.V. Kimel. J. Phys.: Condens. Matter **33**, 075802 (2021).
[19] T.B. Shapayeva, A.R. Yumaguzin, Yu.N. Kurbatova, R.M. Vakhitov, Fizika metallov i metallovedenie **123**, *3*, 284 (2022) (in Russian).
[20] A.K. Zvezdin, Pis'ma v ZhETF **29**, *10*, 605 (1979) (in Russian).
[21] M.V. Chetkin, Yu.N. Kurbatova, T.B. Shapayeva, FTT **52**, *9*, 1795 (2010) (in Russian).
[22] A.K. Zvezdin, Z.V. Gareeva, K.A. Zvezdin, JMMM **509**, 166876 (2020).
[23] A. Malozyomov, J. Slozunsky, Domennye stenki v materialakh c tsilindricheskimi magnitnymi domenami, Mir, M., (1982), 380 p. (in Russian).
[24] M.A. Shamsutdinov, I.Yu. Lomakina, V.N. Nazarov, A.T. Kharisov, Ferro- i antiferrodinamika, Nauka, M., (2009), 455 p. (in Russian).
[25] P.E. Hopkins, M. Ding, J. Poon. J. Appl. Phys. **111**, 103533 (2012).
[26] A.R. Khorsand, M. Savoini, A. Kirilyuk, A.V. Kimel, A. Tsukamoto, A. Itoh, T. Rasing. Phys. Rev. Lett. **108**, 127205 (2012).
[27] C.D. Stanciu, A.V. Kimel, F. Hansteen, A. Tsukamoto, A. Itoh, A. Kirilyuk, T. Rasing. Phys. Rev. B **73**, 220402 (2006).
[28] J.C. Slonczewski. J. Appl.Phys. **45**, *6*, 2705 (1974).

Translated by Ego Translating